



# 一种高精度微芯片用于微环境中细胞温度波动监测\*

赵雪飞<sup>1)</sup> 鄢晚蕾<sup>1,2)\*\*</sup> 尹加文<sup>1)</sup> 管轶华<sup>1)</sup> 金庆辉<sup>1,2)\*\*</sup>

(<sup>1</sup>) 宁波大学信息科学与工程学院, 宁波 315211;

(<sup>2</sup>) 中国科学院上海微系统与信息技术研究所, 传感技术联合国家重点实验室, 上海 200050)

**摘要** 温度是生物体中重要的参数, 准确测量细胞在代谢过程中的温度波动可为更深入地探究细胞的能量产生和扩散过程提供有价值的信息, 从而促进癌症和其他疾病的研究。本文基于微机电加工和微流控技术制备一批可在微环境下监测细胞代谢过程中温度波动的微芯片。微芯片由捕获细胞的C形“微坝”结构、供液体流动的“微缝”和监测温度波动的电极结构组成, 可将细胞培养、温度监测在微芯片上完成。将有细胞贴壁生长的微芯片放置在37°C恒温环境中, 采用恒电流法实时在线连续监测细胞在代谢过程中的温度波动。该芯片共有9个检测单元, 每个单元的检测都是完全独立的, 可同时检测多个结构上的细胞温度波动情况。微芯片的准确度优于0.013°C, 精度为±0.014°C, 响应速度约0.1 s, 不同厚度Ti/Pt温度传感器的温度-电阻之间的线性拟合参数R<sup>2</sup>大于0.999。在(37±0.015) °C的恒温环境下监测细胞, 发现人肺腺癌细胞系(human lung adenocarcinoma cell, H1975)在代谢过程中温度波动的极差(0.173°C)大于肝星状细胞(hepatic stellate cell, HSC)的极差(0.127°C)。癌细胞H1975的平均温度(37.001°C)高于正常细胞HSC的平均温度(36.989°C)。该芯片为细胞代谢监测、药物筛选等方面提供了新的研究平台。

**关键词** 肿瘤细胞监测, 微流控芯片, 细胞温度, 实时监测

**中图分类号** Q65

**DOI:** 10.16476/j.pibb.2020.0400

细胞作为生物体的基本单元, 很多细胞活动以温度变化为标志, 临床实验证明, 因为癌细胞的代谢活动更强, 癌细胞的温度高于正常细胞<sup>[1-2]</sup>。所以监测活细胞的温度可以为细胞病理学和生理学研究提供有价值的信息, 进而有助于进行新颖的治疗和诊断<sup>[3-4]</sup>。细胞的温度波动一般伴随着所有代谢过程, 如细胞分裂、基因表达、酶反应、代谢和病理状态<sup>[5-9]</sup>。主要可以分成两类: 细胞本身的活动引起的温度波动和在外界刺激下产生的反应<sup>[10]</sup>。在高温治疗领域, 精确监测加热程序的温度和肿瘤细胞在高温作用下的温度波动尤其重要, 如果做不到精确监测, 肿瘤细胞周围的健康组织会受到伤害<sup>[11-12]</sup>。降低培养细胞的温度会导致细胞增殖速度降低, 总代谢降低<sup>[13]</sup>。因此活细胞的温度监测不仅可以使我们对细胞代谢有更深入地了解, 还有助于掌握细胞的病理状态, 从而开发出用于某些疾病诊断和治疗的技术<sup>[14]</sup>。

传统的细胞温度监测方法主要有以下几种方法。一种是使用热敏荧光材料进行温度监测, 温度的监测基于热敏荧光材料随温度变化而变化, 如荧光强度<sup>[1]</sup>、荧光带宽<sup>[15]</sup>、荧光寿命<sup>[16]</sup>等。用于发光测量的热敏荧光材料包括纳米颗粒<sup>[17]</sup>、纳米凝胶<sup>[1]</sup>、荧光共聚物<sup>[18]</sup>等。但由于荧光温度计具有多参数敏感性(pH、溶液浓度等), 受环境干扰大, 所以很难精确测定细胞代谢引起的温度波动。另一种是使用探针式温度计测量细胞内的温度<sup>[19]</sup>,

\* 中国国家重点研究发展计划(2017YFA0205303), 浙江省自然科学基金(LQ19F010004), 宁波市自然科学基金(2017A610229), 中国博士后科学基金(2018M642384), 宁波大学“海洋生物技术和海洋工程学科群”和KC Wong Magna基金特殊研究资金资助项目。

\*\* 通讯联系人。

鄢晚蕾 Tel: 17354759296, E-mail: gaowanlei@nbu.edu.cn

金庆辉 Tel: 15825587272, E-mail: jinqinghui@nbu.edu.cn

收稿日期: 2020-11-06, 接受日期: 2021-02-02

将热电偶探针插入细胞内监测细胞温度，使用这种方法会破坏细胞结构从而影响细胞的代谢。

基于荧光检测方法的不稳定性，以及热电偶探针方法会对细胞造成创伤的限制，我们开发出一种微流控芯片来检测细胞在代谢过程中的温度波动。该芯片由具有微通道的细胞培养结构和电极键合而成，共有9个串联的结构单元，结构之间相对独立。该方法灵敏度高、稳定性好、无创，可以实现实时在线连续监测细胞温度波动。

## 1 材料与方法

### 1.1 电极层的制备

采用标准的微机电系统（micro electromechanical system, MEMS）技术制备电极层（图1）。首先将Pyrex7740玻璃清洗干净并干燥，然后在玻璃片上溅射一层厚度为50/100 nm的Ti（粘附层）/Pt，再以1 000 r/min的转速将LC100A光刻胶旋涂30 s，最终在硅片上形成 $(2.4\pm0.1)\mu\text{m}$ 的厚度，光刻显影后得到所需要的图形结构，再采用离子束（IonBeam）加工工艺向下刻蚀150 nm去掉多余的Ti/Pt，等离子去胶后形成由Ti/Pt组成的温度传感器和焊点。最后利用等离子体增强化学气相沉积（PECVD）的方法沉积一层厚度为500 nm的SiO<sub>2</sub>用于绝缘。

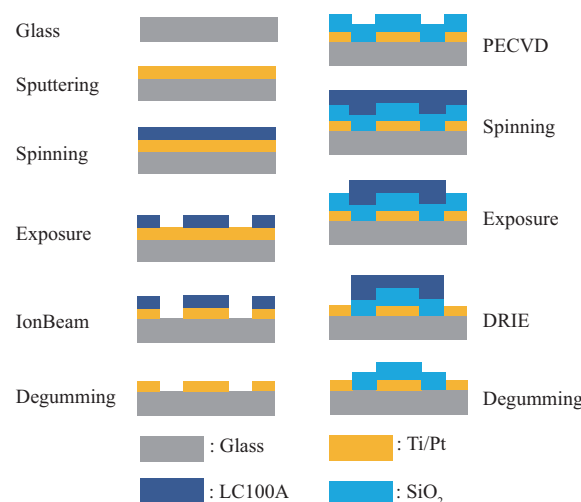


Fig. 1 Flow chart of electrode preparation process

### 1.2 细胞培养层的制备

使用常规的光刻技术制备聚二甲基硅氧烷（PDMS）模具<sup>[20-21]</sup>，首先使用与电极制备同样的方法在干净的硅片上涂一层LC100A光刻胶，光刻显影后利用深反应离子刻蚀（DRIE）在硅片上向

下刻蚀5 μm。使用旋转涂敷法在清洗干净的硅片表面涂上一层厚度为35 μm的SU-83050光刻胶，在水平面上静置2 h后将硅片放在90°C热板上前烘，接下来对准光刻时曝光100 s，再将硅片放在65°C的热板上后烘5 min，然后使用显影液显影并在热板上坚膜，此刻模具制备完成。最后将质量比为10:1的已抽真空PDMS浇筑在模具上，在90°C的烘箱中烘1 h固化，脱模并打孔得到细胞培养层。

### 1.3 键合

准备好已经划片的电极和已切割并打孔的PDMS细胞培养结构，将细胞培养结构有通道的一面和玻璃片上有电极的一面朝上放置，一起放入等离子体清洗器中处理60 s，在键合仪下对准键合，最后放在120°C热板上热键和3 h，这样就完成了整个微流控芯片的制备，图2示微芯片的示意图与实物图。

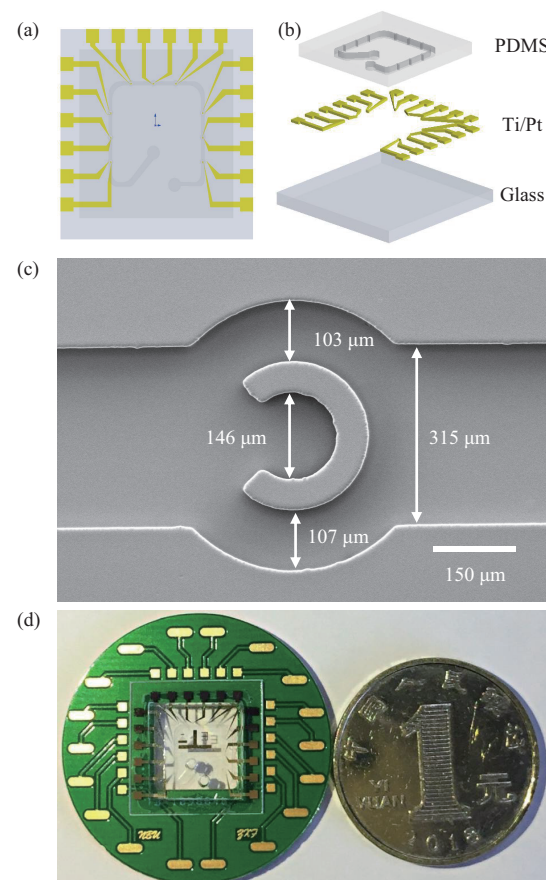


Fig. 2 System diagram of integrated Pt micro-electrode with a microfluidic chip

(a) The image of the microchip integrated with Pt thermo-sensor. The size of the microchip was 2×2 cm. (b) The biochip consisted of a glass substrate, patterned electrodes and PDMS layer. (c) SEM image of the C-shaped dam in the channel. (d) The image of the microchip mounted with the PCB board.

## 1.4 细胞培养

非癌变细胞-肝星状细胞 (HSC) 和肺腺癌细胞 (H1975) 均从中国科学院的细胞库购买。所有细胞均通过了支原体污染测试，并分别在 DMEM (Gibco) 培养基和 RPMI-1640 (Mackiln) 培养基中培养，培养基补充了 10% 胎牛血清 (FBS, Gibco)。每 3 天更换一次培养液，细胞传代两次，以获得足够的细胞供后续实验使用。将芯片放在 120°C 高压蒸汽灭菌锅 (BXM-30R) 中灭菌 30 min，放入 80°C 烘箱中烘干。再把芯片抽真空并进样培养基 (10%FBS+90%DMEM/RPMI-1640)，孵育 24 h。将细胞进样到芯片内，进样口的移液枪枪头注满培养基，在含有 5% CO<sub>2</sub> 的潮湿环境中于 37°C 培养箱中培养 24 h，贴壁生长后进行测量。

## 2 结 果

### 2.1 微芯片设计

为提高细胞的捕获率，该微流控芯片设计 9 个串联 C 形“微坝”检测结构，每个“微坝”结构与玻璃基板的电极之间有 5 μm 高的“微缝”，既能成功拦截细胞，又能使培养基自由流动（图 3）。每个检测结构都能够实现实时在线连续监测细胞温度的波动，且相互之间没有干扰。

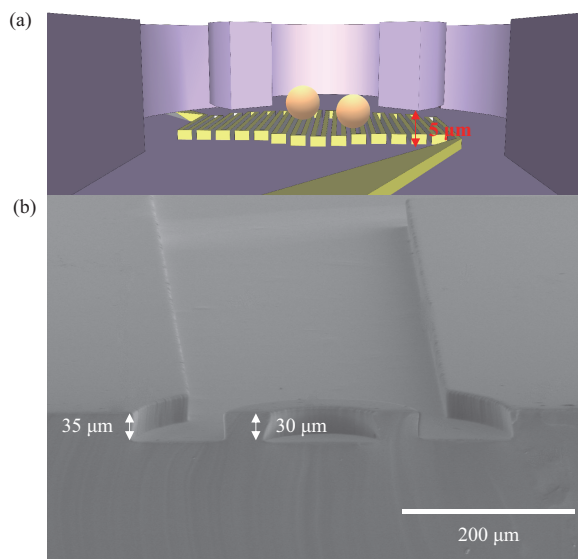


**Fig. 3 Schematic and physical image of the c-type "micro-dam" detection structure**

(a) The height of the “micro-slit” between the c-type “micro-dam” structure and the glass substrate was 5 μm. (b) the channel height of the PDMS microchip was 35 μm, the height of “micro-dam” structure was 30 μm.

## 2.2 校准

根据 Pt 材料的温度-电阻之间良好的线性特性进行校准（表 1）。将芯片放在温度波动为 ±0.015°C 的恒温水箱中固定，将水温依次设置为 20°C、25°C、30°C、35°C、40°C，每个温度值稳定后监测 10 min，通过电化学工作站的恒电流法测得对应温度的电阻。根据设置的恒温水箱温度和测得的电阻值计算出温度-电阻之间的线性关系。表 1 为不同厚度的 Ti/Pt 线性拟合参数，R<sup>2</sup> 均大于 0.999，可用于监测细胞温度的波动。

**Table 1 Linear fitting parameters of Ti/Pt temperature sensors with different thicknesses**

Parameter Number	Intercept	Slope	Pearson's <i>r</i>	Adj. <i>R-Square</i>
1	657.101 62	1.381 55	0.999 93	0.999 83
2	698.790 99	1.505 84	0.999 76	0.999 41
3	713.222 66	1.542 23	0.999 95	0.999 87
4	876.593 00	1.848 93	0.999 97	0.999 93
5	2 088.011 13	4.050 46	0.999 92	0.999 80
6	2 097.085 84	4.072 38	0.999 74	0.999 32
7	2 184.255 38	4.089 34	0.999 94	0.999 85
8	2 185.698 13	4.240 07	0.999 99	0.999 96

## 2.3 准确度与精度

为了高精度监测细胞代谢时的温度变化，温度传感器应具有较好的准确度和精度。将芯片放置于 37°C 恒温水浴中，待环境温度稳定后，传感器的温度波动见图 4，温度波动的最大值为 0.013°C，由此可以得出温度传感器的准确度优于 0.013°C。而平均温度与最大温度和最小温度的差值分别为 0.012°C 和 -0.014°C，表明温度传感器的精度为 ±0.014°C。由此可知该传感器具有较好的准确度和精度。

## 2.4 响应时间与恢复时间

温度传感器的快速响应对实时在线连续监测细胞温度波动有重要的意义（图 5），选择 0°C（冰水混合物）和 37°C（恒温水箱设置）两个时间点，使用电化学工作站以 0.002 s 的频率进行采样。先将温度传感器放在 0°C 冰水混合物中（AB），再快速将传感器移至 37°C 恒温水箱中（BC），测得温度传感器的响应时间为 0.125 s。在 37°C 恒温水浴中监测一段时间（CD），再将芯片转移至 0°C 冰水混合物中（DE），测得恢复时间为 0.134 s。约 0.1 s 的响应时间可以保证该芯片实时在线连续监测细胞在代谢过程中的温度波动。

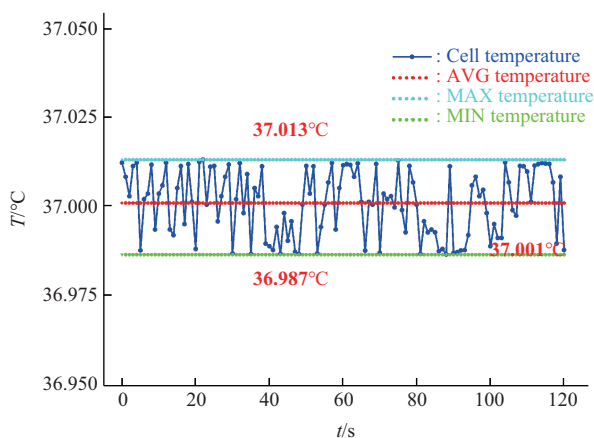


**Fig. 4 Test of accuracy and precision of temperature sensor**

In a 37°C constant temperature water bath, the maximum, minimum and average temperature fluctuations were 37.013°C, 36.987°C and 37.001°C in sequence. It can be seen that the accuracy of the microfluidic chip was better than 0.013°C and the precision was  $\pm 0.014^{\circ}\text{C}$ .

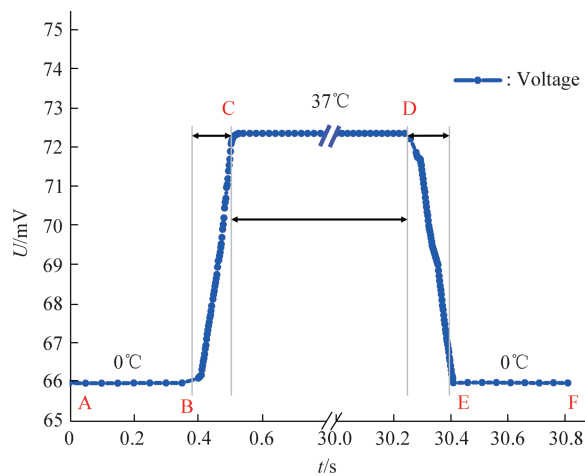


**Fig. 5 Temperature sensor response speed and recovery speed test**

Section AB and EF meant that the chip was placed in a mixture of ice and water at 0°C, and the CD section was that the chip was placed in a constant temperature water bath at 37°C. BC meant the response time of the chip from 0°C to 37°C was 0.125 s. The DE segment indicated that the chip's recovery time from 37°C to 0°C was 0.134 s.

## 2.5 细胞的捕获

芯片包括基板、电极、绝缘层和构造层。简而言之，通过标准 MEMS 工艺来制造电极层，绝缘层是通过 PECVD 制成的，基材由厚度为 400~500  $\mu\text{m}$  的玻璃组成，细胞培养层是通过传统的软

光刻技术制成的，厚度为 35  $\mu\text{m}$ ，C 形“微坝”结构与玻璃基板之间有 5  $\mu\text{m}$  的高度差，高度差小于细胞直径，所以可以用于拦截细胞。

将 H1975 细胞移去培养基，用磷酸缓冲盐溶液 (phosphate buffer saline, PBS) 冲洗一次，再用 10% 的甲醛溶液在室温下固定 20 min。随后使用 DAPI 溶液孵育 30 min，将染色后的细胞进样到微流控芯片内，在吸收波长为 340 nm、发射波长为 488 nm 的荧光显微镜下观察（图 6），发现该 C 形“微坝”结构可以捕获到细胞，再次进样溶液不会对已经拦截的细胞产生影响。可根据目标捕获的细胞数量调整进样细胞的浓度。该方法既能测量到细胞在正常生长代谢时的温度波动又不损害细胞。在复杂的细胞环境中，细胞之间可以在互不干扰的情况下监测到温度的变化具有重要意义<sup>[22]</sup>。

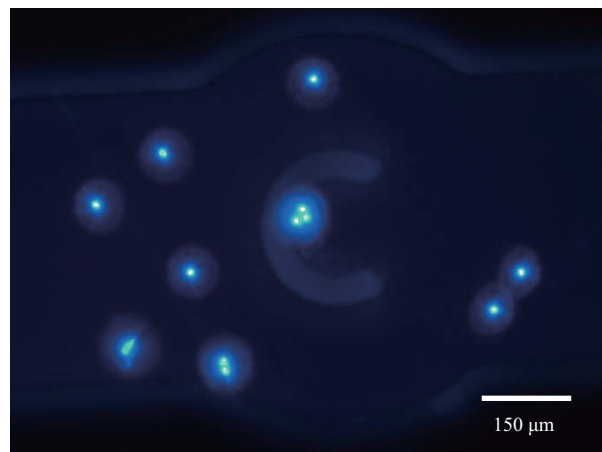


**Fig. 6 Cell capture ability of microfluidic chip**

The H1975 cells stained by DAPI were injected into the microfluidic chip by a pipette through the injection port. Through observation under a fluorescence microscope, the microfluidic chip can capture cells smoothly.

## 2.6 有无HSC、H1975细胞温度波动对比

当 H1975 细胞在芯片内正常贴壁生长时，将合适尺寸的胶管放入芯片的进样口和出样口中，以防止液体流入芯片内影响细胞的生长。将有 H1975 细胞的芯片和只有培养基的空白对照芯片同时放入 37°C 恒温水箱中，测得的温度波动如图 7 所示，H1975 细胞在代谢过程中温度波动范围是 -0.091~0.082°C，在 156 s 时细胞温度达到最低 (36.909°C)，在 176 s 时细胞温度达到最大值 (37.082°C)。而空白芯片的温度波动为  $\pm 0.015^{\circ}\text{C}$ 。

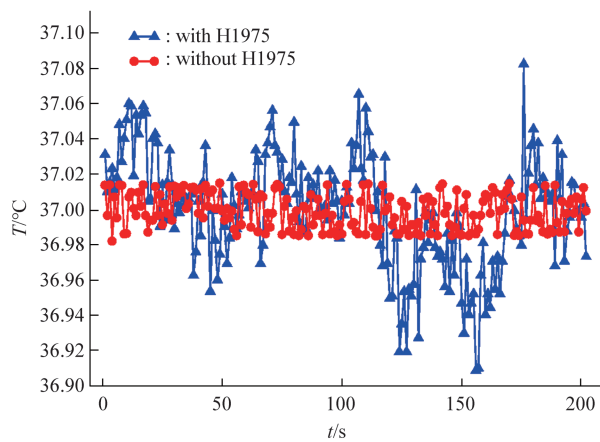


**Fig. 7 Comparison of temperature fluctuation with or without H1975 cells growth in 37°C constant temperature water bath**

The chip with H1975 cells attached to the wall and the chip without cells were placed in the same position in the constant temperature water tank. The same electrochemical workstation was used to measure at the same time.

使用上述方法监测HSC细胞在代谢过程中的温度波动(图8), HSC细胞的温度波动范围是-0.063~0.064°C, 在9 s时温度到达最低(36.937°C), 在90 s时温度达到最高(37.064°C)。而没有细胞的空白芯片温度波动仍在±0.015°C。以上两组空白对照测得的环境温度波动方差均为0.01%, 表明该检测体系提供的环境温度较为稳定, 有利于测定细

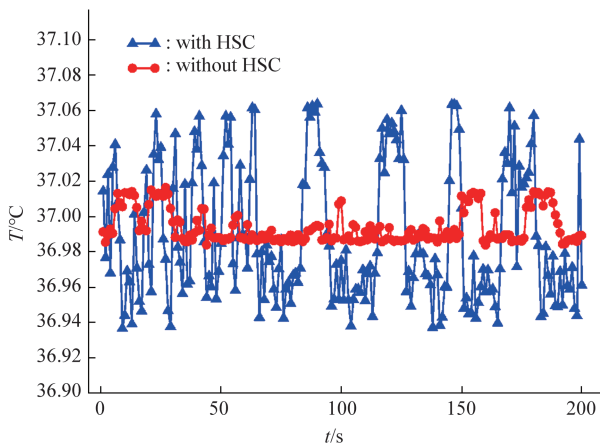


**Fig. 8 Comparison of temperature fluctuation with or without HSCs growth in 37°C constant temperature water bath**

The chip with HSCs attached to the wall and the chip without cells were placed in the same position in the constant temperature water tank. The same electrochemical workstation was used to measure at the same time.

胞代谢引起的微小温度波动。

由癌细胞(H1975)和非癌细胞(HSC)在代谢过程中的温度波动情况(图9)可以看出, 癌细

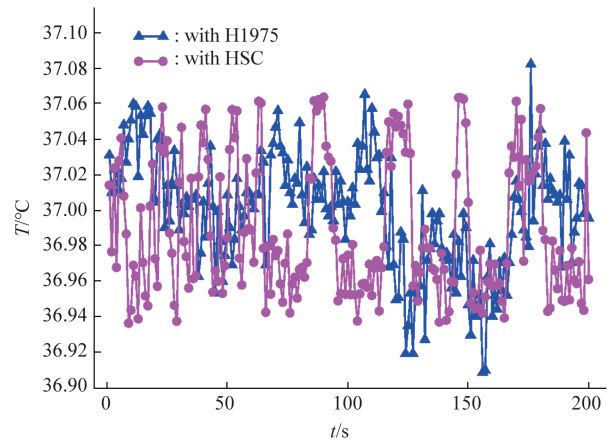


**Fig. 9 Comparison of the temperature fluctuation during the metabolism of H1975 cells and HSCs in a constant temperature environment of 37°C**

The average temperature of H1975 cells is 0.012°C higher than that of HSCs.

胞温度波动的极差为0.173°C(-0.091~0.082°C), 非癌细胞温度波动的极差为0.127°C(-0.063~0.064°C), 由此可知癌细胞在代谢过程中温度波动比非癌细胞大。H1975细胞在代谢时的平均温度(37.001°C)高于HSC的平均温度(36.989°C), 两种细胞平均温度的差值为0.012°C, 其中H1975细胞在监测的200 s内有110 s的温度波动大于0°C, 而HSC仅有70 s的温度大于0°C, 所以癌细胞代谢能力更强, 温度也比非癌细胞更高。因此该芯片能够高精度监测多种细胞在代谢过程中的温度波动, 反映细胞实时的生理状态, 对于细胞生理学与病理学研究具有重要意义。

### 3 讨 论

我们开发了一种集成高精度薄膜铂热电阻的微流控芯片, 实现了片上培养细胞, 并且实时在线连续监测细胞代谢过程的温度波动。将一定浓度的细胞悬浮液进样到芯片内, 通过C形“微坝”结构将细胞捕获在铂热电阻上, 并在芯片内进行细胞培养。根据结果可知, 该芯片的电阻-温度在线性拟合过程中 $R^2$ 均大于0.999, 准确度优于0.013°C, 精度为±0.014°C。在C形“微坝”结构成功捕获细胞的

情况下，癌细胞H1975和非癌细胞HSC在代谢时的温度波动分别为 $-0.091\sim-0.082^{\circ}\text{C}$ 和 $-0.063\sim0.064^{\circ}\text{C}$ ，而没有细胞的芯片温度波动为 $\pm0.015^{\circ}\text{C}$ ，癌细胞H1975的平均温度比非癌细胞HSC的平均温度高 $0.012^{\circ}\text{C}$ ，因此该芯片足以监测细胞在代谢时的温度波动。这种测量细胞代谢过程中温度波动的方法和芯片结构的设计为将来单细胞温度监测的研究奠定了坚实的基础，能够在制药过程中获取更多细胞代谢活性的信息，可以在更长的时间内连续无创地观察细胞代谢参数。

## 参 考 文 献

- [1] Goto C, Okabe K, Funatsu T, et al. Hydrophilic fluorescent nanogel thermometer for intracellular thermometry. *J Am Chem Soc*, 2009, **131**(8): 2766-2767
- [2] Gavriloia G V, Hurdic A, Ghimigean A M, et al. Spatial-temperature high resolution map for early cancer diagnosis. *Proceedings of SPIE*, 2009, **7171**: 71710W-1
- [3] Lucia U, Grazzini G, Montruccio B, et al. Constructal thermodynamics combined with infrared experiments to evaluate temperature differences in cells. *Sci Rep*, 2015, **5**: 11587
- [4] Vetrone F, Naccache R, Zamarrón A, et al. Temperature sensing using fluorescent nanothermometers. *Acs Nano*, 2010, **4**(6): 3254-3258
- [5] Binslem S A, Ahmad M R, Awang Z. Intracellular thermal sensor for single cell analysis-short review. *Jurnal Teknologi*, 2015, **73**(6): 71-80
- [6] Sakaguchi R, Kiyonaka S, Mori Y. Fluorescent sensors reveal subcellular thermal changes. *Curr Opin Biotechnol*, 2015, **31**: 57-64
- [7] Lowell B B, Spiegelman B M. Towards a molecular understanding of adaptive thermogenesis. *Nature*, 2000, **404**(6778): 652-660
- [8] Himm-Hagen J. Cellular thermogenesis. *Annu Rev Physiol*, 1976, **38**: 315-351
- [9] Tanaka E, Yamamura M, Yamakawa A, et al. Microcalorimetric measurements of heat production in isolated rat brown adipocytes. *Biochem Int*, 1992, **26**(5): 873-877
- [10] Donner J S, Thompson S A, Alonso-Ortega C, et al. Imaging of plasmonic heating in a living organism. *Acs Nano*, 2013, **7**(10): 8666-8672
- [11] Moreau D, Lefort C, Burke R, et al. Rhodamine B as an optical thermometer in cells focally exposed to infrared laser light or nanosecond pulsed electric fields. *Biomed Opt Express*, 2015, **6**(10): 4105-4117
- [12] Maestro L M, Haro-González P, del Rosal B, et al. Heating efficiency of multi-walled carbon nanotubes in the first and second biological windows. *Nanoscale*, 2013, **5**(17): 7882-7889
- [13] Yoon S K, Song J Y, Lee G M. Effect of low culture temperature on specific productivity, transcription level, and heterogeneity of erythropoietin in Chinese hamster ovary cells. *Biotechnol Bioeng*, 2003, **82**(3): 289-298
- [14] Bai T, Gu N. Micro/nanoscale thermometry for cellular thermal sensing. *Small*, 2016, **12**(34): 4590-4610
- [15] Benayas A, Escuder E, Jaque D. High-resolution confocal fluorescence thermal imaging of tightly pumped microchip Nd: YAG laser ceramics. *Appl Phys B*, 2012, **107**(3): 697-701
- [16] Okabe K, Inada N, Goto C, et al. Intracellular temperature mapping with a fluorescent polymeric thermometer and fluorescence lifetime imaging microscopy. *Nature Commun*, 2012, **3**: 705
- [17] Arai S, Ferdinandus, Takeoka S, et al. Micro-thermography in millimeter-scale animals by using orally-dosed fluorescent nanoparticle thermosensors. *Analyst*, 2015, **140**(22): 7534-7539
- [18] Hayashi T, Fukuda N, Uchiyama S, et al. A cell-permeable fluorescent polymeric thermometer for intracellular temperature mapping in mammalian cell lines. *PLoS One*, 2015, **10**(2): e0117677
- [19] Wang C, Xu R, Tian W, et al. Determining intracellular temperature at single-cell level by a novel thermocouple method. *Cell Res*, 2011, **21**(10): 1517-1519
- [20] Mcmillan K S, Mccluskey A G, Sorensen A, et al. Emulsion technologies for multicellular tumour spheroid radiation assays. *Analyst*, 2015, **141**(1): 100-110
- [21] Whitesides G M, Ostuni E, Takayama S, et al. Soft lithography in biology and biochemistry. *Annu Rev Biomed Eng*, 2001, **3**: 335-373
- [22] Albertini D F, Anderson E. The appearance and structure of intercellular connections during the ontogeny of the rabbit ovarian follicle with particular reference to gap junctions. *J Cell Biol*, 1974, **63**(1): 234-250

## Monitoring Cell Temperature Fluctuation in Microenvironment Chip With a High-precision Microchip<sup>\*</sup>

ZHAO Xue-Fei<sup>1)</sup>, GAO Wan-Lei<sup>1,2)\*\*</sup>, YIN Jia-Wen<sup>1)</sup>, GUAN Yi-Hua<sup>1)</sup>, JIN Qing-Hui<sup>1,2)\*\*</sup>

(<sup>1</sup>)Faculty of Electrical Engineering and Computer Science, Ningbo University, Ningbo 315211, China;

(<sup>2</sup>)State Key Laboratories of Transducer Technology, Shanghai Institute of Microsystem and Information Technology, Chinese Academy of Sciences, Shanghai 200050, China)

**Abstract** Temperature is an important parameter in organisms. Accurate measurement of cellular temperature fluctuations in the metabolic process can provide valuable information for more in-depth exploration of the energy production and diffusion process of cells, thereby promoting the research of cancer and other diseases. In this study, integrated microchips were fabricated in batch based on Micro-Electro-Mechanical System and microfluidic technology, which can monitor temperature fluctuations in a microenvironment during the process of cell metabolism. The microchip is composed of a C-shaped “micro-dam” structure, a “micro-slit” for liquid flow, and an electrode structure, which can complete cell culture and temperature monitoring on a microchip. The microchip with adherent cells was placed in a constant temperature environment of 37°C, and the constant current method was used to continuously real-time monitor the temperature changes of the cells in the metabolic process. The chip has a total of 9 detection units, each of which was completely independent and applied for detecting multiple cells’ temperature fluctuation parallelly. The accuracy and precision of the microchip were respectively better than 0.013°C and ±0.014°C with 0.1 s response speed. The linear fitting parameter  $R^2$  between temperature and resistance of Ti/Pt temperature sensors of different thicknesses was greater than 0.999. Different cells trapped by this microchip were cultured on chip and monitored under a constant temperature environment of (37±0.01)°C. The temperature fluctuation range of human lung adenocarcinoma cell (H1975) (0.173°C) during metabolism was greater than that of hepatic stellate cell (HSC) (0.127°C). The average temperature of cancer cells H1975 (37.001°C) is higher than that of normal HSCs (36.989°C). In conclusion, this integrated microchip provides a tool of real-time monitoring cell temperature variation for the study of cell physiology and pathology.

**Key words** tumor cell monitoring, microfluidic chip, cellular temperature, real-time monitor

**DOI:** 10.16476/j.pibb.2020.0400

\* This work was supported by grants from the National Key Research and Development Program of China (2017YFA0205303), Natural Science Foundation of Zhejiang Province (LQ19F010004), Natural Science Foundation of Ningbo City (2017A610229), China Postdoctoral Science Foundation (2018M642384), Ningbo University’s “Marine Biotechnology and Ocean Engineering Discipline Group” and Special Research Funding from the KC Wong Magna Fund.

\*\* Corresponding author.

GAO Wan-Lei. Tel: 86-17354759296, E-mail: gaowanlei@nbu.edu.cn

JIN Qing-Hui. Tel: 86-15825587272, E-mail: jinqinghui@nbu.edu.cn

Received: November 6, 2020 Accepted: February 2, 2021